Growth and magnetism of ultrathin Fe films on Pt(100)

K. He,[1] L. J. Zhang,[1] X. C. Ma,[1] J. F. Jia,[1] Q. K. Xue,[1,*] and Z. Q. Qiu[2]
[1]*Beijing National Laboratory for Condensed Matter Physics, Institute of Physics, Chinese Academy of Sciences, Beijing 100080, China*
[2]*Department of Physics, University of California at Berkeley, Berkeley, CA 94720, USA*
(Received 6 April 2005; revised manuscript received 16 August 2005; published 26 October 2005)

The scanning tunneling microscopy, low energy electron diffraction, and surface magneto-optic Kerr effect are used to investigate the morphology, structure, and magnetism of ultrathin Fe films on a Pt(100) surface. At room temperature, the deposited Fe atoms exchange sites with the Pt atoms of the substrate, and then grow in a quasi layer-by-layer mode. The Fe films show in-plane anisotropy for all coverages (up to 7 ML). Annealing at 600 K switches the easy magnetization axis from in-plane to perpendicular when the thickness is smaller than 5.2 ML. The coercivity increases gradually to its maximum at 3.3 ML and then decreases abruptly, accompanied with a surface structure transition from (1×1) to $c(2\times2)$. These results demonstrate the formation of Fe-Pt $L1_0$ and $L1_2$ chemically ordered alloys and a phase transition between them. The atom exchange process is found to play a key role in the alloy formation at significantly reduced growth temperature.

DOI: 10.1103/PhysRevB.72.155432 PACS number(s): 75.30.Gw, 75.70.Ak, 75.70.Rf

I. INTRODUCTION

Dimension reduction in magnetic materials could lead to dramatic changes in their magnetic properties such as anisotropies, moments, and critical behaviors.[1] Magnetic ultrathin films grown on nonmagnetic substrates have been a subject of extensive studies in the past fifteen years in hopes of improving our understanding on low-dimensional magnetism.[1,2] Fe films are of special interest because face-centered-cubic (fcc) Fe that only exists above its magnetic ordering temperature in bulk may be stabilized at room temperature in a form of ultrathin films. Rich structural and magnetic properties have been observed in the Fe films grown on different substrates.[3–10]

Similar surface energies of Fe ($2.9\ \mathrm{Jm^{-2}}$) and Pt ($2.7\ \mathrm{Jm^{-2}}$)[1] make the growth of epitaxial Fe films on Pt substrate relatively easy. The atomic nearest neighbor distance of the Pt(100) surface is 2.77 Å, in between that of the body-centered-cubic (bcc) (2.86 Å) and fcc (2.54 Å) Fe(100) surface, and thus, complex structural properties could be expected in Fe films on the Pt(100) surface. Moreover, the magnetic moments of Pt atoms could be induced by adjacent Fe atoms that incorporate the strong spin-orbit coupling of Pt into Fe films,[11–14] which leads to interesting magnetic phenomena.

Up to now, there have been few studies on Fe films grown on Pt(100) substrate. On the contrary, many studies have been devoted to Fe films on (100) surface of Pd which has similar lattice constant and electronic structure with Pt, showing complex structural and magnetic properties. The Fe films on Pd(100) grown at low temperature show perpendicular magnetic anisotropy below 2.5 ML, while the films deposited at room temperature exhibit in-plane anisotropies for all thicknesses.[15] Structural analyses for the Fe films grown at room temperature reveal that the films above 5 ML are body-centered-tretragonal (bct) a distorted bcc structure,[16] and those below 4 ML are disordered face-centered-tetragonal (fct) FePd alloy which was supposed to contribute to the in-plane anisotropy.[17] Fe films on Pd(100) show magnetism even in a submonolayer regime, which is different from those on many other substrates, e.g., Cu(100) and Ag(100).[4] A comparison between Fe/Pd(100) and Fe/Pt(100) could help to clarify these complex phenomena.

The strong spin-orbit coupling in Pt in Fe/Pt multilayers or $L1_0$ ordered alloys leads to strong magnetic crystalline anisotropies and magneto-optic effects, which makes them very promising for magnetic storage.[18,19] Along this line, the structure and magnetism of Fe/Pt multilayers were studied extensively. The Fe/Pt(100) multilayers prepared by molecular beam epitaxy (MBE) show in-plane magnetic anisotropy and the Fe layers transform from fcc like to bcc phase when the thickness is larger than 8 Å.[20,21] However, grazing incidence x ray scattering studies indicate[22] that the "fcc" Fe is actually Fe-Pt alloy layers resulting from the atom diffusion to the Fe layers from the Pt overlayers. What is more interesting in Fe/Pt(100) multilayers is that the FePt $L1_0$ ordered alloy can be obtained by annealing at only about 600 K,[23,24] a temperature much lower than in traditional methods, which makes the preparation of FePt $L1_0$ alloy more efficient. The relative low activation energy of atomic interdiffusion at Fe/Pt interface was directly correlated to the phenomenon observed.[25] However, the mechanism for the lower activation energy is still not clear.

In this work, by using scanning tunneling microscopy (STM), low energy electron diffraction (LEED), and surface magneto-optic Kerr effect (SMOKE), we have investigated the morphology, structure, and magnetic property of both as deposited and annealed Fe films on the Pt(100) surface. We'll show that the Fe films grown at room temperature exhibit in-plane magnetic anisotropy and hysteresis only after 2.2 ML. Annealing at 600 K leads to the formation of ordered Fe-Pt alloys which exhibit perpendicular magnetic anisotropy. The intermixing caused by the atomic exchange process at the interface is found to be responsible for these magnetic properties.

II. EXPERIMENT

Our experiments were carried out in a multifunctional ultrahigh vacuum (UHV) system equipped with a commercial

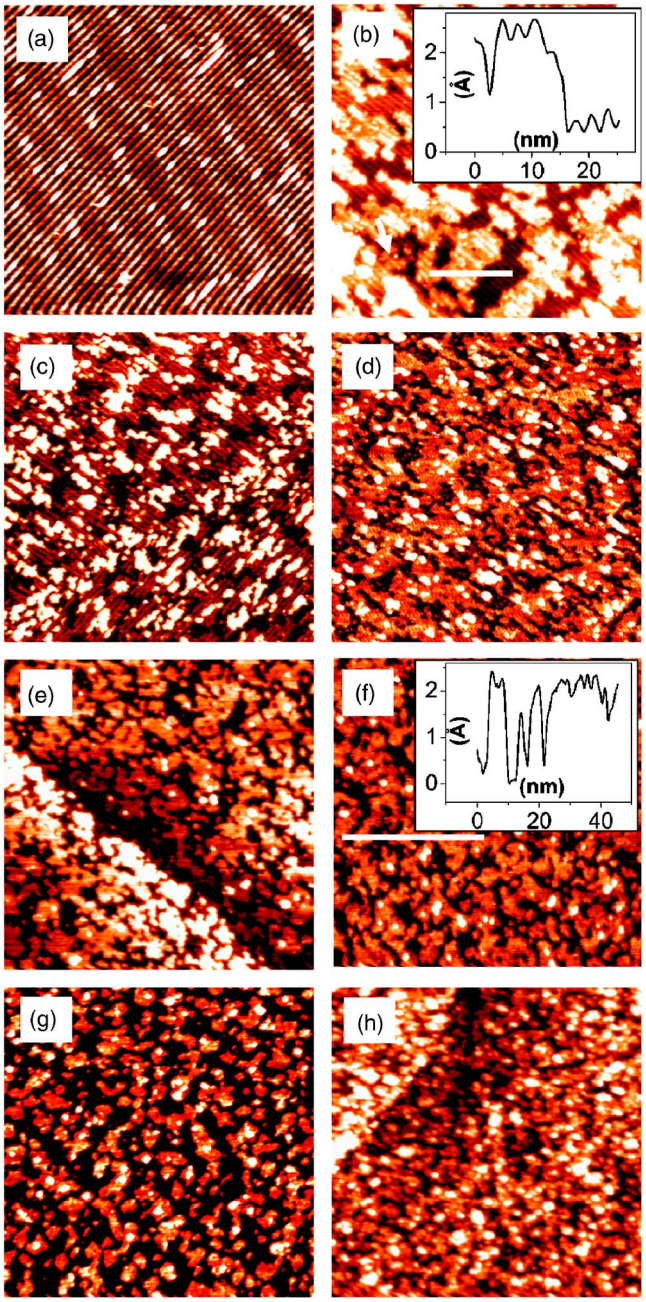

FIG. 1. (Color online) STM images of as-grown Fe films on the Pt(100) surface with different coverage: (a) A clean surface of Pt(100) (50 nm×50 nm), (b) 0.6 ML (100 nm×100 nm), (the marked line profiles are shown in the inset) (c) 1.2 ML (100 nm ×100 nm), (d) 1.8 ML (100 nm×100 nm), (e) 2.6 ML (100 nm ×100 nm), (f) 3.8 ML (100 nm×100 nm), (the marked line profiles are shown in the inset) (g) 6.0 ML (100 nm×100 nm), and (h) 7.5 ML (100 nm×100 nm).

OMICRON variable temperature STM, LEED,[26] and a homemade SMOKE. The SMOKE setup is similar to that described in Ref. 27. The magnetic field was generated by two pairs of electromagnets perpendicular to each other in the UHV chamber. Both polar and longitudinal hysteresis loops can be obtained without rotating the sample. The maximal magnetic field is 1000 Oe.

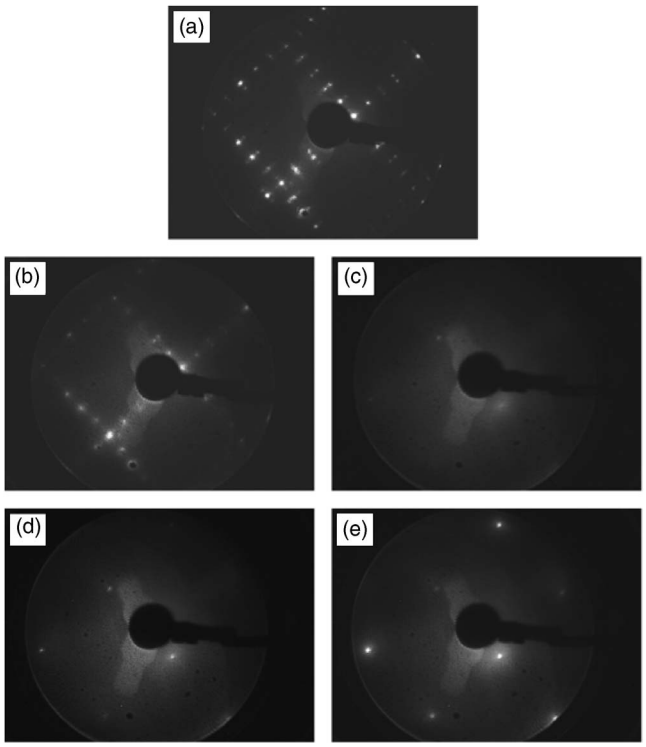

FIG. 2. LEED patterns of as-deposited Fe films on the Pt(100) surface at different coverage. (a) A clean surface of Pt(100), (b) 0.6 ML, (c) 1.5 ML, (d) 2.6 ML, and (e) 3.5 ML.

The Pt(100) single crystal surface was cleaned by cycles of Ar ion sputtering at 1 KeV and annealing at ~1000 K. The clean surface is characterized by sharp fivefold LEED spots and by STM images with well-defined row like (5×29) reconstruction. Fe was evaporated from a resistively heated Ta boat. The Fe coverage was calibrated by STM images, since the Fe films grow on Pt(100) in a quasi layer-by-layer mode, as shown below. Wedge-shaped samples are used in SMOKE measurements to obtain a reliable dependence of magnetic properties versus thickness, avoiding possible coverage fluctuation in different experiments. The wedge samples were made by moving the substrate out of a Ta shutter gradually. A very thick film ("shoulder") was deposited first at the edge of the substrate before moving, so that the depositing time at a certain position of the wedge can be estimated in SMOKE measurements. The STM images reported here were recorded at constant current mode with a tunneling current of 20 pA to 100 pA. The LEED patterns were taken with a beam energy of 70 eV. Kerr ellipticity was acquired as the magnetic signal in SMOKE measurements. All of the measurements were carried out at room temperature.

III. RESULTS AND DISCUSSION

A. As-deposited films

The clean surface of Pt(100) exhibits a row like (5×29) reconstruction, as shown by the STM image in Fig. 1(a). The rows are along a [011] or [01-1] direction, separated from

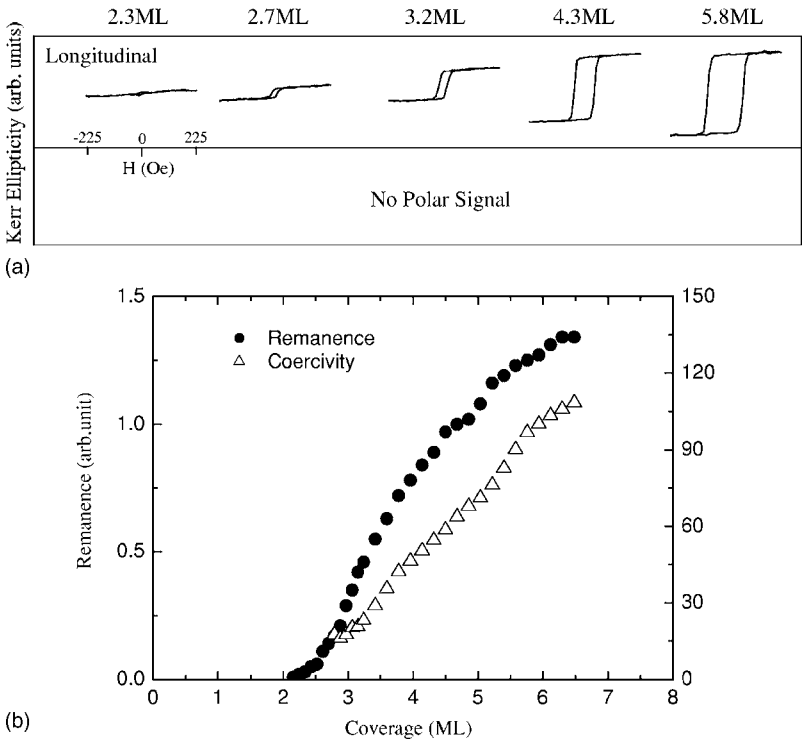

FIG. 3. (a) The representative hysteresis loops of the as-deposited Fe films. (b) The measured remanence and coercivity as a function of thickness for the as-deposited Fe films.

each other by 14 Å, nearly five times of the surface lattice constant. This reconstruction has a very complex, nearly incommensurate structure resulting from the formation of a buckled hexagonal layer on top of the square lattice of the substrate,[28] usually termed as Pt(100) hex. The overall surface has a (5×29) symmetry, as indicated by the LEED pattern in Fig. 2(a).

The STM images of the Fe films with different coverages, deposited at room temperature, are displayed in Fig. 1. At 0.6 ML [see Fig. 1(b)], more than half of the surface is covered with islands with irregular shapes. Row like reconstructions very similar to that of Pt(100) can be discerned on most of the islands. The distance between neighboring rows and the contrast of rows is the same to that of the Pt substrate, and the island height is also the same to the step height on the clean Pt(100) surface. Using different bias voltages won't change these results. So, we can conclude that these reconstructed islands are Pt islands. The steps of the surface remain straight after Fe deposition, so the additional Pt atoms for growth of the islands should come from the Pt terrace.

Similar phenomenon was ever reported in Fe/Au(100) and was attributed to the atomic site exchanges between Fe and Au atoms in the substrate.[29,30] Since Pt and Au are adjacent in the periodic table of the elements and their (100) surfaces have very similar reconstructions, it is reasonable that the atomic exchange also occurs in the Fe/Pt(100). The Fe atoms landing on the Pt(100) surface, after a short time of terrace diffusion, will exchange sites with the Pt atoms in the substrate. With increasing number of Pt atoms on the surface, the Pt atoms will nucleate into reconstructed islands, in a manner similar to Pt homoepitaxy.[31]

Atomic exchange processes are common in heteroepitaxy of metals.[32–34] The deposited metal with higher surface energy than the substrate metal tend to enter subsurface to reduce their surface area, and decrease the system energy. This process can take place even at room temperature.[32] Fe has a larger surface energy than Pt, and Fe, Pt are well miscible. So the deposited Fe atoms favor exchanging with Pt atoms over direct nucleation on the surface.

From the present STM images, we can't find explicit evidences of the presence of Fe atoms on surface. The possible reason is that Fe atoms scatter in the Pt matrix, rather than form subsurface islands, which might be easy to be discerned. *Ab initio* calculations have shown that Fe atoms favor random distribution in (100) surface of 5 d metals.[35] According to a previous study,[29] Fe atoms in the Au substrate remain isolated and appear in STM images as very dim depressions. Considering the fact that Pt has a closer metallic radius with Fe, it is difficult to distinguish Fe and Pt atoms in the STM images.

From STM images we find that the area covered by Pt islands is nearly the same to the Fe coverage, suggesting that one Fe atom replaces one Pt atom on average. It is different with Fe/Au(100), where the observed island area is about three times that of the Fe coverage.[29] The difference may be due to different exchange mechanisms. In Fe/Au(100), it was proposed that Fe atoms place themselves in the hollow sites of the underling square lattices, ejecting on average the three adjacent Au atoms.[29] In Fe/Pt(100), based on this observation, Fe atoms should occupy the position of the second layer Pt atoms, and one Fe atom exchanges with one Pt atom on average. It is reasonable since this site is the same to the Fe position in the Fe-Pt $L1_0$ ordered alloy that is a thermodynamically stable phase.

At 1.2 ML [see Fig. 1(c)], the original surface is nearly covered with one monolayer Pt, on which some unreconstructed islands are formed. At 1.8 ML [Fig. 1(d)], these unreconstructed islands grow, and meanwhile, islands of next

layer appear. Above 2 ML [Fig. 1(e)] the film grows in a quasi layer-by-layer mode, which can be seen from the line profile in Fig. 1(f), where the height variation of the surface is limited to two atomic layers. From the line profile, we can also observe that the height fluctuation of terraces is relatively large (~0.3 Å) compared with Fe films on other surfaces (<0.2 Å). With increasing film thickness, the coverage threshold of a layer the islands of next layer decrease gradually, which makes the morphology rougher. At 7.5 ML, the surface is characterized by small clusters [Fig. 1(h)]. However, the height fluctuation doesn't exceed 3.5 Å.

The typical LEED patterns at coverage of 0.6 ML, 1.5 ML, 2.6 ML, and 3.5 ML are shown in Fig. 3, respectively. At 0.6 ML [Fig. 2(b)], except that the fractional-order spots become a little bit weaker, the overall LEED pattern is very similar with that of the clean Pt(100) surface. With increasing Fe coverage, both the fractional and integral spots weaken gradually and background intensity increase at the same time. From 1.2 ML to 1.8 ML, the diffraction patterns are almost invisible, as shown in Fig. 2(c). Similar phenomena were also observed in Fe/Pd(100)[16,17] and Fe/Au(100).[36,30] The formation of disordered layers was argued to be responsible. Above 1.8 ML, the 1×1 pattern recovers and remains for all higher coverages [Figs. 2(d) and 2(e)]. The size of the diffraction spots increases gradually with the increasing coverage, which is consistent with the formation of the smaller islands observed by STM.

The results of the SMOKE measurement are summarized in Fig. 3. From the thickness dependent remanence of the samples, we can observe that the remanence of longitudinal loops appear at ~2.2 ML and increase monotonically with increasing thickness, while the polar signal never appears. It indicates that the easy magnetic axis of the as-deposited Fe films is in-plane for all coverages studied. The coercivity also increases with thickness and reaches 110 Oe at 6.5 ML.

A universal behavior of perpendicular magnetic anisotropy (PMA) has been observed in Fe films, e.g., fcc Fe(100) on Cu(100),[3] bcc Fe(100) on Au(100),[3] and Ag(100).[4] On Pd(100) surface, Fe films formed at low temperature show PMA below 2.5 ML, while the films grown at room temperature exhibit in-plane anisotropy for all thicknesses.[15] The quantitive LEED and surface extended x-ray absorption fine structure study[17] has demonstrated that the Fe films below 4 ML grown at room temperature are actually disordered fct FePd alloy, which is responsible for the in-plane magnetic anisotropy. Similar to Pd, Fe also has good miscibility with Pt, so intermixing is also likely to happen. Our STM observation of the Pt islands also suggests the intermixing at room temperature. The relative large terrace height fluctuation indicates that the surface of the film is not composed of only one element. The step height of ~1.8 Å measured at 3.8 ML is much larger than the interplanar spacing of bcc Fe(100), instead is very close to that of disordered FePt alloy. In Fe/Pt(100) multilayers, fcc like phases caused by alloying with Pt atoms was observed.[22] So, the observed in-plane magnetic anisotropy should be associated with the formation of disordered Fe-Pt alloy.

In this experiment, the Fe films show hysteresis after 2.2 ML, which means that the Curie temperature exceeds room temperature at a thickness as small as ~2 ML. The critical thickness is close to that of the Fe films on Cu(100) and Ag(100),[4] but much larger than the Fe films on Pd(100) which even show submonolayer magnetism at room temperature.[15] The origin of such a difference is still not clear. The hybridization between the electrons of substrate and Fe atoms was supposed to be responsible for the difference.[3,37] In Fe/Pd(100), the magnetic moments of the Pd atoms can be induced by the hybridization with neighboring Fe atoms, which contribute to long-range magnetic order even when Fe atoms are isolated, while some other substrates suppress the moments of Fe atoms. Pt has similar electronic structure with Pd. The induced Pt moments by neighboring ferromagnetic atoms have been confirmed by many experiments.[11–14] Similar behavior should be observed in the present case. However, only induced moments are not sufficient to establish long-range magnetic order. The coupling between induced magnetic moments has to be strong enough so that the long range order won't be destroyed by thermal fluctuation, namely, the Curie temperature of the diluted Fe alloy must exceed the measurement temperature. The Curie temperatures of disordered Pt-rich Fe-Pt alloys are close to room temperature, and decrease drastically with

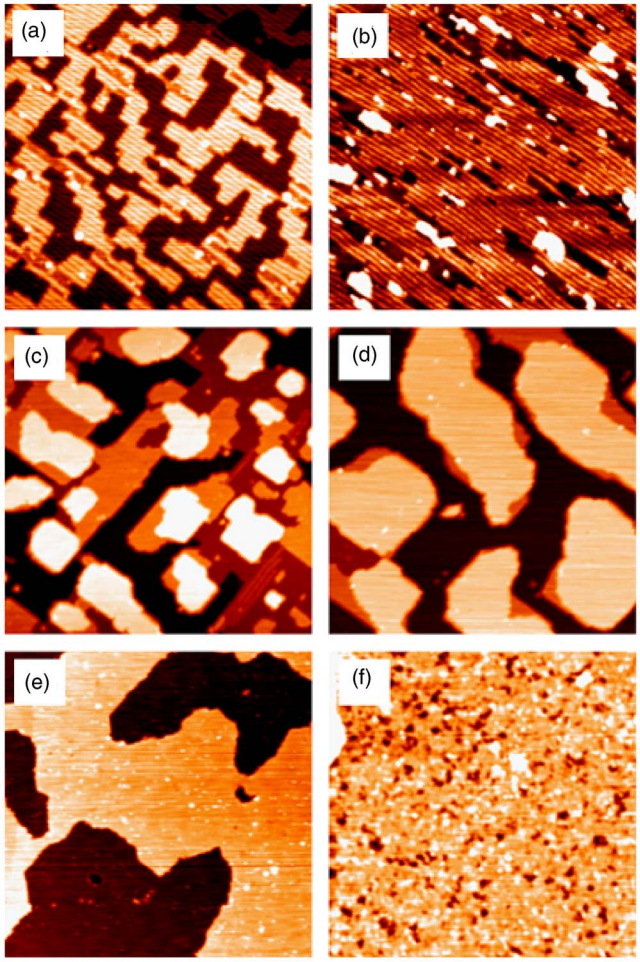

FIG. 4. (Color online) The STM images (100 nm×100 nm) of the Fe films after annealing at 600 K for 30 min: (a) 0.6 ML, (b) 1.2 ML, (c) 1.5 ML, (d) 2.0 ML, (e) 2.6 ML, and (f) 4.8 ML.

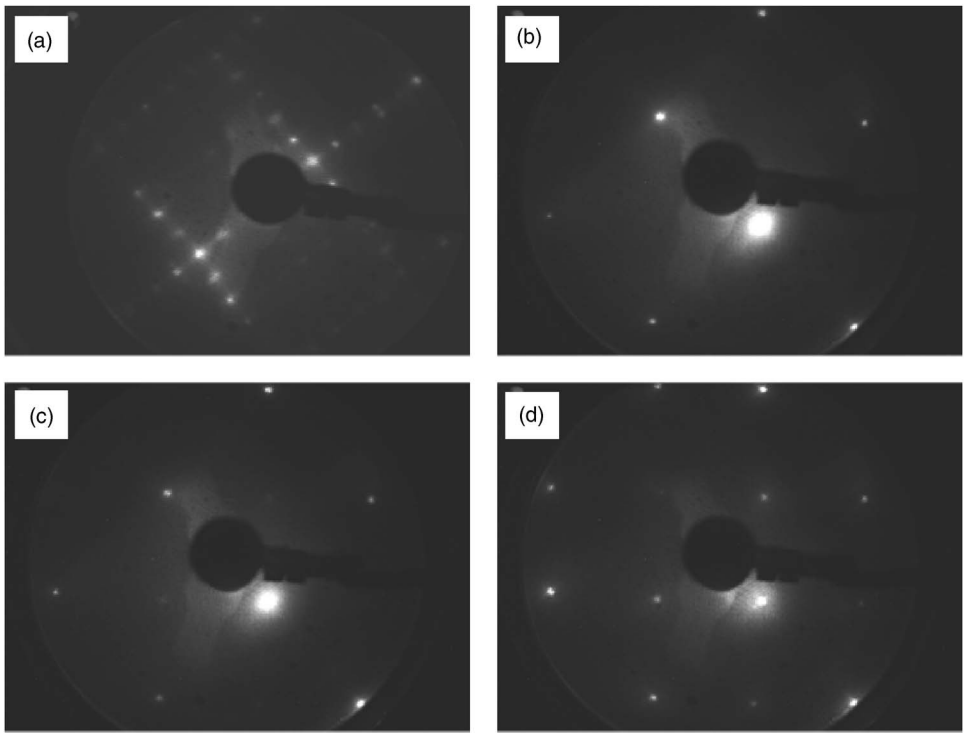

FIG. 5. LEED patterns of the Fe films after annealing at 600 K for 30 min. (a) 0.6 ML, (b) 1.5 ML, (c) 2.6 ML, and (d) 3.5 ML.

decreasing Fe/Pt ratio,[38] while the Curie temperature of Pd-rich Fe-Pd disordered alloy is around 400~500 K.[39] So, Therefore, we speculate that at ~1 ML, the moments of Pt atoms are most likely induced by adjacent Fe atoms, but they fail to be coupled ferromagnetically to establish a hysteresis at room temperature.

B. Annealed films

After annealing the samples at 600 K for 30 min, significant changes in the morphology, LEED patterns, and magnetism were observed. Figure 4 shows the morphologies of the annealed Fe films of different thicknesses. At 0.6 ML and 1.2 ML [Fig. 4(a) and 4(b)], the islands become more ordered and maintain the characteristic row like reconstruction of the Pt(100). Small unreconstructed areas can also be observed. At higher coverage, the morphology becomes rough and multileveled. As shown in Fig. 4(c), for the 1.5 ML sample four levels can be observed over a range of 200 nm $\times$200 nm. From the remained reconstruction, which is on the islands of the first layer, we know that the lowest level exposed is the original substrate. Interestingly, for higher coverage, no fifth level is seen before completion of the fourth level. At 2.0 ML [Fig. 4(d)], all islands have a thickness of three layers. When the coverage reaches to 2.6 ML, the surface becomes flat again [see Fig. 4(e)]. The smooth morphology essentially remains for all higher coverages studied [see Fig. 4(f)].

The corresponding LEED patterns (Fig. 5) of the annealed samples basically agree with the STM observation. After annealing, the films show a well-defined (1×1) diffraction pattern, and the disordered phase for the as-deposited samples was not observed. A new observation is that at 3.3 ML, a phase transition from (1×1) to $c(2\times2)$ occurs [Fig. 5(d)]. The annealing also leads to significant changes in magnetism. The typical hysteresis loops and the evolution of remanence with thickness are shown in Fig. 6. The polar signal appears at as early as 1.8 ML, which indicates that the easy axis switches to the direction perpendicular to the surface. The coercivity from the hysteresis loops is much larger (>1250 Oe at 2.9 ML, since the maximal field of our system is not large enough to saturate the sample) than before annealing. At 3.0 ML the hysteresis loop develops into a stepped structure. This kind loop suggests that two uncoupled phases with different coercivities simultaneously contribute to the magnetic signals. With increasing Fe coverage, the magnetic signal from the phase with smaller coercivity becomes stronger while that with larger coercivity becomes weaker. At 4.2 ML, a normal loop with a coercivity of ~150 Oe is observed, and thus the contribution from the phase with larger coercivity vanishes. From the samples with uniform thicknesses in the same coverage range, we didn't obtained hysteresis loops with steps (not shown), which further supports that two different phases contribute to the SMOKE signals due to the large laser beam size. Hence we conclude that at ~3.3 ML a phase with large coercivity transforms to another phase with small coercivity. Above 4.2 ML, the polar signal starts to decrease meanwhile the longitudinal signal appears and increases with increasing thickness. The results clearly indicate that a spin reorientation transition (SRT) takes place. After 5.2 ML, the polar signal disappears gradually, and the easy axis becomes in-plane.

The SMOKE results indicate that annealing leads to the PMA of the Fe films below 5.2 ML. It seems contrary to the case of the Fe/Pd(100) system where intermixing leads to the in-plane anisotropy,[15,17] since annealing will enhance intermixing. However, besides intermixing enhancement, annealing can also bring on other effects, for example, the for-

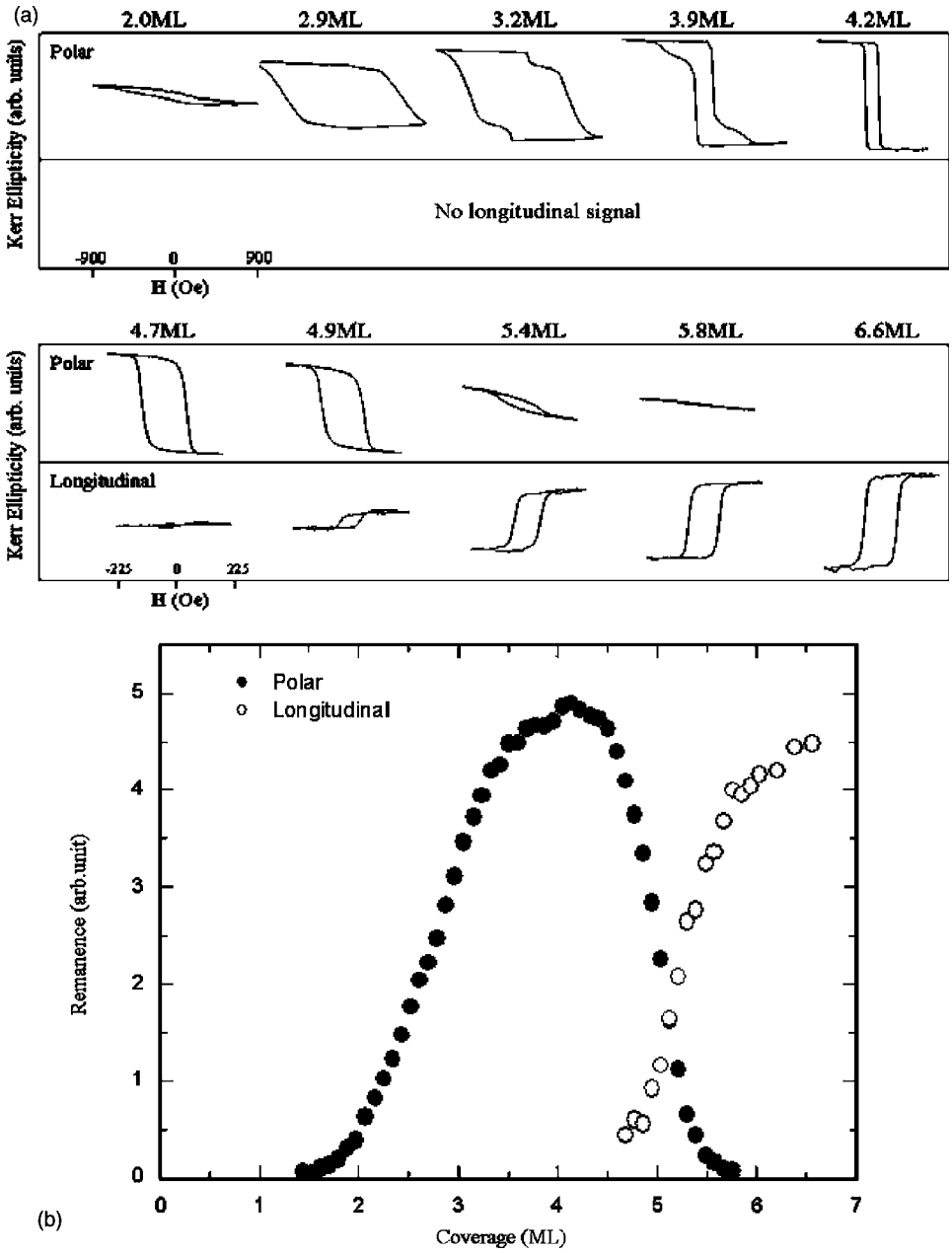

FIG. 6. (a) The representative hysteresis loops of the Fe films after annealing. (b) The measured remanence as a function of the thickness for the Fe films after annealing.

mation of thermodynamically more stable ordered alloys. Unfortunately, there is no *in situ* tool in our system to characterize the crystallographic structure of the films directly. Nevertheless, we believe that it is the Fe-Pt ordered alloys that contribute to the complex structural and magnetic properties of the annealed films based on the comparison between our data and previous results. The reasons are listed below.

(1) The Fe(100) surface does not show $c(2\times2)$ reconstruction. Oxygen can induce $c(2\times2)$ reconstruction on the Fe(100) surface by dissociation of CO molecules or by oxygen adsorption.[40,41] In the case of oxygen adsorption, at least one Langmuir O_2 is needed to induce the $c(2\times2)$ reconstruction,[41] while the base pressure of our system is 5×10^{-11} Torr, which excludes the possibility of oxygen contamination. Therefore, the $c(2\times2)$ pattern must come from some structure composed of Fe and Pt, rather than from the pure Fe deposited, strongly suggesting that the interface mixing of Fe and Pt does take place.

(2) According to the binary phase diagram, Fe and Pt are miscible at any ratio, and ordered alloys are thermodynamically stable phases. Surface effects, according to the theoretical calculation in Ref. 42, won't make a difference in this system. So ordered alloys tend to form upon annealing. Similar behavior was reported in the Mn/Pt(100) system where bulk like Pt_3Mn ordered alloy could be formed by annealing Mn films on the Pt(100) surface.[43] Besides, interface interdiffusion upon annealing at around 600 K was also reported in Co/Pt(100)[44] and Pt/Fe(100).[45]

(3) The Fe-Pt ordered alloys can explain the observed structural and magnetic properties of the films. There are three ordered Fe-Pt alloy phases.[38] Equiatomic FePt is an $L1_0$ type that consists of alternately stacking (100) atomic

planes of the two elements. So, in [100] direction it has the same lateral structure with the bulk terminated Pt(100) and will show a 1×1 diffraction pattern. Fe_3Pt and $FePt_3$ are an $L1_2$ type that is fcc lattice with the face center positions occupied by the majority atoms. The different atoms at the face centers make the primitive vectors of the (100) planes of this structure rotate by 45° and elongated to $\sqrt{2}$ times of the original ones, giving rise to a $c(2\times2)$ superstructure. $FePt_3$ is antiferromagnetic with a Néel temperature below room temperature,[46] so it should be excluded from the present discussion. FePt and Fe_3Pt are both ferromagnetic, while FePt has a much larger magnetic crystalline anisotropy than Fe_3Pt.[47] The easy axis of FePt is along its stacking direction, i.e., [100] direction. So the ordered FePt $L1_0$(100) alloy films could show PMA. Perpendicular magnetic anisotropy induced by the formation of ordered alloy has been reported in annealed Fe/Pt(100) multilayers[23] and co-evaporated FePt(100) alloy.[48] For Fe_3Pt, although it is isotropic in bulk, when grown on the Pt(100) surface, the tensile stress and surface anisotropy can also lead to PMA. There is no intermediate phase between the two alloy phases, so with increasing Fe composition the FePt phase can transit to the Fe_3Pt phase directly, which will be accompanied by a dramatic decrease in coercivity and the transition of the LEED pattern from 1×1 to $c(2\times2)$.

(4) Previously we studied the Co/Pt(100) system under similar experimental conditions with this experiment,[49] and also observed in-plane magnetic anisotropy before annealing and perpendicular magnetic anisotropy after annealing. However, we didn't observe the abrupt decrease in the coercivity and the corresponding change from 1×1 to $c(2\times2)$ by LEED. It is understandable since there is no Co_3Pt $L1_2$ phase according to the Co-Pt phase diagram. The absence of both the $c(2\times2)$ and $L1_2$ phase once again strongly suggests the structure transition of the alloys.

The formation of ordered alloys suggests that the Pt atoms can diffuse long enough to reach thermodynamically stable positions at the low annealing temperature of 600 K. The transition from the equiatomic alloy to the Fe-rich alloy suggests that only a certain amount of Pt atoms participate in the alloying process. The diffusion of most Pt atoms in the substrate is kinetically limited at this temperature, and these atoms are not actually active. What leads to the difference between the "active" Pt atoms and the "inactive" Pt atoms? We argue that the "active" Pt atoms are those exchanged with initially deposited Fe atoms. Based on our discussions above, the exchanged Pt atoms form the disordered alloy films with the Fe atoms. There should be many defects in the films due to its disordered nature and the existence of strain, more significant diffusion should be expected compared to the Pt single crystal, which makes the formation of the ordered alloys kinetically possible.

IV. SUMMARY

We have studied the growth, structure, and magnetism of ultrathin Fe films on the Pt(100) surface. We found that room temperature is high enough for the initially deposited Fe atoms to exchange with the substrate Pt atoms. Subsequent Fe atoms grow in a quasi layer-by-layer mode into a disordered alloy film. The as-deposited Fe films exhibit an in-plane anisotropy for all coverages. After annealing at 600 K, FePt $L1_0$ ordered alloy forms between 1.2 ML and 3.3 ML showing PMA with a coercivity as large as 1250 Oe. When the Fe coverage is larger than 3.3 ML, the FePt $L1_0$ phase transforms to the Fe_3Pt $L1_2$ phase with smaller coercivity. Above 5.2 ML, an SRT takes place and the easy magnetization axis switches to in-plane. The atomic exchange is shown to play the key role in the formation of the ordered alloys with decreased growth temperature.

ACKNOWLEDGMENTS

This work is financially supported by NSF and MOST of China. Z. Q. Q. is grateful for the support of NSF Grant No.DMR-0405259.

*Electronic address: qkxue@aphy.iphy.ac.cn

[1] F. J. Himpsel, J. E. Ortega, G. J. Mankey, and R. F. Willis, Adv. Phys. **47**, 511 (1998).
[2] J. Shen and J. Kirschner, Surf. Sci. **500**, 300 (2002).
[3] C. Liu and S. D. Bader, J. Vac. Sci. Technol. A **8**, 2727 (1990).
[4] D. P. Pappas, C. R. Brundle, and H. Hopster, Phys. Rev. B **45**, R8169 (1992).
[5] J. Thomassen, F. May, B. Feldmann, M. Wuttig, and H. Ibach, Phys. Rev. Lett. **69**, 3831 (1992).
[6] R. Allenspach and A. Bischof, Phys. Rev. Lett. **69**, 3385 (1992).
[7] P. Ohresser, J. Shen, J. Barthel, M. Zheng, Ch. V. Mohan, M. Klaua, and J. Kirschner, Phys. Rev. B **59**, 3696 (1999).
[8] Z. Q. Qiu, J. Pearson, and S. D. Bader, Phys. Rev. Lett. **70**, 1006 (1993).
[9] H. J. Elmers, J. Hauschild, H. Höche, U. Gradmann, H. Bethge, D. Heuer, and U. Köhler, Phys. Rev. Lett. **73**, 898 (1994).
[10] J. Krebs, B. Jonker, and G. Prinz, J. Appl. Phys. **61**, 2596 (1987).
[11] T. Koide, T. Shidara, K. Yamaguchi, A. Fujimori, H. Fukutani, N. Nakajima, T. Sugimoto, T. Katayama, and Y. Suzuki, Phys. Rev. B **53**, 8219 (1996).
[12] M. Finazzi, L. Braicovich, C. Roth, F. U. Hillebrecht, H. B. Rose, and E. Kisker, Phys. Rev. B **50**, 14 671 (1994).
[13] G. Schütz, R. Wienke, W. Wilhelm, W. B. Zeper, H. Ebert, and K. Spörl, J. Appl. Phys. **67**, 4456 (1990).
[14] H. Maruyama, A. Koizumi, K. Kobayashi, and H. Yamazaki, Jpn. J. Appl. Phys., Suppl. **32-2**, 290 (1993).
[15] C. Liu and S. D. Bader, J. Appl. Phys. **67**, 5758 (1990).
[16] J. Quinn, Y. S. Li, H. Li, D. Tian, F. Jona, and P. M. Marcus, Phys. Rev. B **43**, 3959 (1991).
[17] C. Boeglin, H. Bulou, J. Hommet, X. Le Cann, H. Magnan, P. Le Fevre, and D. Chandesris, Phys. Rev. B **60**, 4220 (1999).
[18] C. H. Lee, R. F. C. Farrow, C. J. Lin, E. E. Marinero, and C. J. Chien, Phys. Rev. B **42**, 11384 (1990).
[19] A. Ceblollada, R. F. C. Farrow, and M. F. Toney, in *Magnetic*

Nanostructures, edited by H. S. Nalwa, p. 93 (American Scientific Publisher, 2002).
[20] M. Sakurai, Phys. Rev. B **50**, 3761 (1994).
[21] M. Sakurai, N. Imamura, K. Hirano, and T. Shinjo, J. Magn. Magn. Mater. **147**, 16 (1995).
[22] T. C. Hufnagel, M. C. Kautzky, B. J. Daniels, and B. M. Clemens, J. Appl. Phys. **85**, 2609 (1999).
[23] B. M. Lairson, M. R. Visokay, R. Sinclair, and B. M. Clemens, Appl. Phys. Lett. **62**, 639 (1993).
[24] Y. Endo, N. Kikuchi, O. Kitakami, and Y. Shimada, J. Appl. Phys. **89**, 7065 (2001).
[25] Y. Endo, K. Oikawa, T. Miyazaki, O. Kitakami, and Y. Shimada, J. Appl. Phys. **94**, 7222 (2003).
[26] J. F. Jia, X. Liu, J. Z. Wang, J. L. Li, X. S. Wang, Q. K. Xue, Z. Q. Li, Z. Zhang, and S. B. Zhang, Phys. Rev. B **66**, 165412 (2002).
[27] Z. Q. Qiu and S. D. Bader, Rev. Sci. Instrum. **71**, 1243 (2002).
[28] G. Ritz, M. Schmid, P. Varga, A. Borg, and M. Rønning, Phys. Rev. B **56**, 10518 (1997).
[29] O. S. Hernán, A. L. Vázquez de Parga, J. M. Gallego, and R. Miranda, Surf. Sci. **415**, 106 (1998).
[30] V. Blum, C. Rath, S. Müler, L. Hammer, K. Heinz, J. M. García, J. E. Ortega, J. E. Prieto, O. S. Hernán, J. M. Gallego, A. L. Vázquez de Parga, and R. Miranda, Phys. Rev. B **59**, 15 966 (1999).
[31] T. R. Linderoth, J. J. Mortensen, K. W. Jacobsen, E. Lægsgaard, I. Stensgaard, and F. Besenbacher, Phys. Rev. Lett. **77**, 87 (1996).
[32] S.-L. Chang, J.-M. Wen, P. A. Thiel, S. Günther, J. A. Meyer, and R. J. Behm, Phys. Rev. B **53**, 13747 (1996).
[33] S. Rousset, S. Chiang, D. E. Fowler, and D. D. Chambliss, Phys. Rev. Lett. **69**, 3200 (1992).
[34] J. Shen, J. Giergiel, A. K. Schmid, and J. Kirschner, Surf. Sci. **328**, 32 (1995).
[35] V. S. Stepanyuk and W. Hergert, Phys. Rev. B **62**, 7542 (2000).
[36] A. M. Begley, S. K. Kim, J. Quinn, F. Jona, H. Over, and P. M. Marcus, Phys. Rev. B **48**, 1779 (1993).
[37] F. Wilhelm, U. Bovensiepen, A. Scherz, P. Poulopoulos, A. Ney, H. Wende, G. Ceballos, and K. Baberschke, J. Magn. Magn. Mater. **222**, 163 (2000).
[38] B. Predel, in *Landolt-Börnstein-Group IV Physical Chemistry*, Vol. 5, SubVol. E, Fe-*Pt* (*Iron-Platinum*) (Springer-Verlag, Berlin, 1995).
[39] G. Longworth, Phys. Rev. **172**, 572 (1968).
[40] A. Kirilyuk, J. Giergiel, J. Shen, M. Straub, and J. Kirschner, Phys. Rev. B **54**, 1050 (1996).
[41] A. Kirilyuk, J. Giergiel, J. Shen, and J. Kirschner, Phys. Rev. B **52**, R11672 (1995).
[42] A. Christensen, A. V. Ruban, P. Stoltze, K. W. Jacobsen, H. L. Skriver, J. K. Nørskov, and F. Besenbacher, Phys. Rev. B **56**, 5822 (1997).
[43] W. Kim, S. C. Hong, J. Seo, S.-J. Oh, H. G. Min, and J.-S. Kim, Phys. Rev. B **70**, 174453 (2004).
[44] C. Boeglin, A. Barbier, B. Carrière, R. Cousandier, J. P. Deville, F. Scheurer, and C. Speisser, Surf. Sci. **251/252**, 602 (1991).
[45] G. W. R. Leibbrandt, R. van Wijk, and F. H. P. M. Habraken, Phys. Rev. B **47**, 6630 (1993).
[46] R. L. Compton, M. J. Pechan, S. Maat, and E. E. Fullerton, Phys. Rev. B **66**, 054411 (2002).
[47] H. Zeng, J. Li, J. P. Liu, Z. L. Wang, and S. Sun, Nature (London) **420**, 395 (2002).
[48] A. Cebollada, D. Weller, J. Sticht, G. R. Harp, R. F. C. Farrow, R. F. Marks, R. Savoy, and J. C. Scott, Phys. Rev. B **50**, 3419 (1994).
[49] M. H. Pan, K. He, L. J. Zhang, J. F. Jia, Q. K. Xue, and Z. Q. Qiu (unpublished).